Reflection Asymmetric Target Detection Based on Correlation Coefficients

Ken Yoong LEE*, Soo Chin LIEW, Santo Valenti SALINAS and Kim Hwa LIM

Centre for Remote Imaging, Sensing and Processing, National University of Singapore

10 Lower Kent Ridge Road, Block S17, Level 2, Singapore 119076

*crslky@nus.edu.sg

Abstract: *This paper explores the use of multiple correlation coefficient and complex correlation coefficient for reflection symmetry testing in multi-look polarimetric synthetic aperture radar (PolSAR) data. The recently proposed block-diagonality test statistic is actually related to the former. The reflection asymmetric target detection was examined using ALOS-2 PALSAR-2 quad-polarisation data, covering two separate test sites in Southeast Asia. Meanwhile, quantitative assessment was reported by employing simulated PolSAR data through Monte-Carlo method. The experimental results confirmed the usefulness of reflection symmetry property of geophysical media, particularly in detecting man-made objects, such as bridges, slightly oriented buildings, vessels, aquaculture farms, etc.*

Keywords: *Complex correlation coefficient, complex Wishart distribution, multiple correlation coefficient, polarimetric synthetic aperture radar, reflection symmetry*

Introduction

Scattering symmetry is of practical importance in crosstalk calibration (van Zyl, 1990) and model-based physical scattering decomposition (Freeman and Durden, 1998). Its potential application for man-made target detection has been noticeably explored. In the literature, target symmetry and its effect on depolarised echo can be traced back to a quarterly progress report submitted by the Ohio State University Research Foundation (1952, Appendix). Four decades later, Nghiem *et al*. (1992) presented an in-depth investigation on symmetric properties of geophysical media encountered in polarimetric remote sensing due to reflection, rotation, azimuthal, and centrical symmetry groups. Other relevant discussions on this aspect for PolSAR also appear in Borgeaud *et al*. (1987), Nghiem *et al*. (1993), Yueh *et al*. (1994), Bringi and Chandrasekar (2001), Lee and Pottier (2009), Cloude (2010), *etc*.

To detect covariance symmetries within multi-look PolSAR images, Pallotta *et al*. (2017) introduced a framework by utilising model order selection. They compared four different model order selectors, namely, Akaike information criterion, generalised information criterion, Bayesian information criterion, and exponentially embedded families. Their framework was then extended by Tahraoui *et al*. (2018) for polarimetric SAR interferometry. More recently, Connetable *et al*. (2022) made use of statistical test for independence in evaluating reflection symmetry in multi-look PolSAR data. They derived the so-called block-diagonality test statistic, where its asymptotic distribution under null hypothesis is a chi-squared distribution. Keeping all these in mind, this paper aims to examine reflection symmetry by using correlation coefficients for man-made target detection in multi-look PolSAR data. Firstly, the mathematical relationship between the block-diagonality test statistic and multiple correlation coefficient is investigated. Secondly, the applicability of multiple correlation coefficient and complex correlation coefficient is studied for reflection symmetry testing.

Reflection Symmetry

In L-look PolSAR data, each pixel can be represented by a 3×3 polarimetric covariance matrix:

$$\mathbf{C} = \begin{bmatrix} \langle |s_{\mathrm{HH}}|^2 \rangle & \langle s_{\mathrm{HH}} s_{\mathrm{HV}}^* \rangle & \langle s_{\mathrm{HH}} s_{\mathrm{VV}}^* \rangle \\ \langle s_{\mathrm{HV}} s_{\mathrm{HH}}^* \rangle & \langle |s_{\mathrm{HV}}|^2 \rangle & \langle s_{\mathrm{HV}} s_{\mathrm{VV}}^* \rangle \\ \langle s_{\mathrm{VV}} s_{\mathrm{HH}}^* \rangle & \langle s_{\mathrm{VV}} s_{\mathrm{HV}}^* \rangle & \langle |s_{\mathrm{VV}}|^2 \rangle \end{bmatrix}, \quad (1)$$

where s_{rt} refers to the scattering element of the received polarisation r and the transmitted polarisation t. The subscripts H and V represent separately horizontal and vertical polarisations. The angular brackets $\langle \, . \, \rangle$ refer to the ensemble average, while the superscript * denotes the complex conjugate. As pointed out by Lee *et al*. (1994), the Hermitian matrix $\mathbf{W} = L\mathbf{C}$ can be assumed to follow a trivariate central complex Wishart distribution (Goodman, 1963):

$$f(\mathbf{W}) = \frac{|\mathbf{W}|^{L-3}}{|\mathbf{\Sigma}|^{L}\pi^{3}\Gamma(L)\Gamma(L-1)\Gamma(L-2)} \exp\{-\mathrm{tr}(\mathbf{\Sigma}^{-1}\mathbf{W})\}, \tag{2}$$

where $|\,.\,|$ and tr denote separately the matrix determinant and trace. $\Gamma(.)$ refers to the gamma function and exp represents the exponential function. The population covariance matrix can be written as

$$\mathbf{\Sigma} = \begin{bmatrix} \sigma_{HH}^{2} & \rho_{HHHV}\sigma_{HH}\sigma_{HV} & \rho_{HHVV}\sigma_{HH}\sigma_{VV} \\ \rho_{HHHV}^{*}\sigma_{HH}\sigma_{HV} & \sigma_{HV}^{2} & \rho_{HVVV}\sigma_{HV}\sigma_{VV} \\ \rho_{HHVV}^{*}\sigma_{HH}\sigma_{VV} & \rho_{HVVV}^{*}\sigma_{HV}\sigma_{VV} & \sigma_{VV}^{2} \end{bmatrix}. \tag{3}$$

Both symbols σ and ρ denote the population standard deviation and complex correlation coefficient, respectively.

Under reflection symmetry assumption, the polarimetric covariance matrix takes the following form:

$$\mathbf{C}_{rs} = \begin{bmatrix} \langle |s_{HH}|^{2} \rangle & 0 & \langle s_{HH}s_{VV}^{*} \rangle \\ 0 & \langle |s_{HV}|^{2} \rangle & 0 \\ \langle s_{VV}s_{HH}^{*} \rangle & 0 & \langle |s_{VV}|^{2} \rangle \end{bmatrix}, \tag{4}$$

where the co- and cross-polarisation channels are uncorrelated, i.e.,

$$\langle s_{HH}s_{HV}^{*} \rangle = \langle s_{HV}s_{VV}^{*} \rangle = 0. \tag{5}$$

In this case, the above covariance matrix consists of only five independent real-valued elements compared to that of nine elements in (1). By rewriting and partitioning the covariance matrix in (4) as

$$\mathbf{C}_{rs} = \begin{bmatrix} \langle |s_{HV}|^{2} \rangle & 0 & 0 \\ 0 & \langle |s_{HH}|^{2} \rangle & \langle s_{HH}s_{VV}^{*} \rangle \\ 0 & \langle s_{VV}s_{HH}^{*} \rangle & \langle |s_{VV}|^{2} \rangle \end{bmatrix} = \begin{bmatrix} \mathbf{C}_{11} & \mathbf{0} \\ \mathbf{0} & \mathbf{C}_{22} \end{bmatrix}, \tag{6}$$

the block-diagonality test statistic, which was derived by Connetable *et al*. (2022) for the reflection symmetry test, is given by

$$Q = \left(\frac{|\mathbf{C}|}{|\mathbf{C}_{11}||\mathbf{C}_{22}|} \right)^{L}. \tag{7}$$

The asymptotic distribution of $-2\,\rho_{bd}\,\ln Q$ under H_0: $\mathbf{\Sigma}_{21} = \mathbf{0}$ is a chi-squared distribution, where ln denotes the natural logarithm and ρ_{bd} is defined in Connetable *et al*. (2022, p. 2879). The vector $\mathbf{\Sigma}_{21}$ is given by

$$\mathbf{\Sigma}_{21} = \begin{bmatrix} \rho_{HHHV}\sigma_{HH}\sigma_{HV} \\ \rho_{HVVV}^{*}\sigma_{HV}\sigma_{VV} \end{bmatrix}. \tag{8}$$

Multiple Correlation Coefficient

Multiple correlation coefficient arises from multiple linear regression (Mudholkar, 2006). It measures the maximum correlation between one random variable and any linear function of other variables (Johnson *et al*., 1994, Chapter 32). The block-diagonality test statistic is, in fact, related to multiple correlation coefficient R:

$$\frac{|\mathbf{C}|}{|\mathbf{C}_{11}||\mathbf{C}_{22}|} = 1 - \frac{\mathbf{C}_{12}\mathbf{C}_{22}^{-1}\mathbf{C}_{21}}{\mathbf{C}_{11}} = 1 - R^2 \tag{9}$$

with

$$\mathbf{C}_{12} = \begin{bmatrix} \langle s_{\mathrm{HV}} s_{\mathrm{HH}}^* \rangle & \langle s_{\mathrm{HV}} s_{\mathrm{VV}}^* \rangle \end{bmatrix} \tag{10}$$

and

$$\mathbf{C}_{21} = \begin{bmatrix} \langle s_{\mathrm{HH}} s_{\mathrm{HV}}^* \rangle \\ \langle s_{\mathrm{VV}} s_{\mathrm{HV}}^* \rangle \end{bmatrix}. \tag{11}$$

Through Cholesky decomposition, it is easy to check that the left side in (9) is bounded between zero and one.

Based on Theorem 3.6 in Anderson *et al*. (1995, p. 44), the squared multiple correlation R^2 for a 3×3 polarimetric covariance matrix under H_0: $\mathbf{\Sigma}_{21} = \mathbf{0}$ is found to be beta-distributed as

$$f(R^2) = \frac{\Gamma(L)}{\Gamma(L-2)} R^2 (1 - R^2)^{L-3}. \tag{12}$$

Its exact distribution depends only on the number of looks L. As derived in Appendix A, the limiting distribution of LR^2 is a gamma distribution with unit scale parameter and a shape parameter of two, when L tends to infinity. The corresponding non-null distribution was previously given by (1.11) in Goodman (1963, p. 155).

Complex Correlation Coefficient

Apart from multiple correlation coefficient, one may test the reflection symmetry in multi-look PolSAR data using pairwise ordinary correlation coefficient, i.e., complex correlation coefficient. By considering 2×2 HH-HV sample covariance matrix

$$\mathbf{C} = \begin{bmatrix} \langle |s_{\mathrm{HH}}|^2 \rangle & \langle s_{\mathrm{HH}} s_{\mathrm{HV}}^* \rangle \\ \langle s_{\mathrm{HV}} s_{\mathrm{HH}}^* \rangle & \langle |s_{\mathrm{HV}}|^2 \rangle \end{bmatrix}, \tag{13}$$

then HH-HV complex correlation coefficient is given by

$$r_{\mathrm{HHHV}} = \frac{\langle s_{\mathrm{HH}} s_{\mathrm{HV}}^* \rangle}{\sqrt{\langle |s_{\mathrm{HH}}|^2 \rangle \langle |s_{\mathrm{HV}}|^2 \rangle}}. \tag{14}$$

Following Fujikoshi *et al*. (2010, pp. 73–74) for a bivariate central complex Wishart distribution, the exact distribution of magnitude squared of complex correlation coefficient under H_0: $\rho_{\mathrm{HHHV}} = 0$ is a beta distribution:

$$f(|r_{\mathrm{HHHV}}|^2) = \frac{\Gamma(L)}{\Gamma(L-1)} (1 - |r_{\mathrm{HHHV}}|^2)^{L-2}. \tag{15}$$

Likewise, its non-null distribution was given by (1.11) in Goodman (1963, p. 155). Noteworthily, similar statistical finding applies to 2×2 HV-VV sample covariance matrix. As the number of looks tends to infinity, Appendix B shows that the magnitude squared of complex correlation coefficient under a certain transformation is exponential distributed with a unit rate parameter. Moreover, it can be proven straightforwardly from (15) that $-\ln(1 - |r_{\mathrm{HHHV}}|^2)$ has also an exponential distribution with a rate parameter of $L - 1$.

Methodology

In this study, the reflection symmetry in multi-look PolSAR data was tested by using separately the aforementioned multiple correlation coefficient and complex correlation coefficient. Figures 1 and 2 present the processing flowchart based on both the correlation coefficients, respectively. No additional speckle suppression was performed using spatial filters (such as Lee refined filter, bilateral filter, *etc*.) in the workflow. The reflection symmetry testing was examined on simulated PolSAR data and ALOS-2 PALSAR-2 quad-polarisation data.

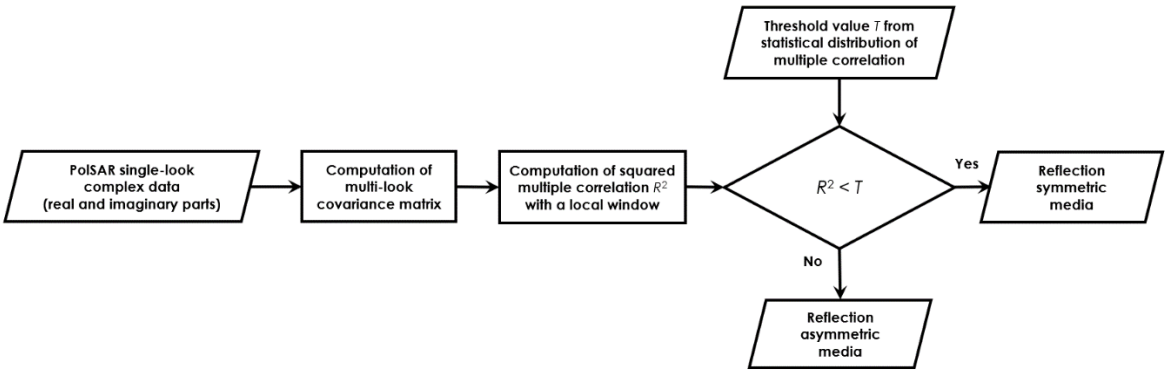

Figure 1: Reflection symmetry testing based on multiple correlation coefficient, where critical value or threshold is determined from (12) with a user-specified significance level α.

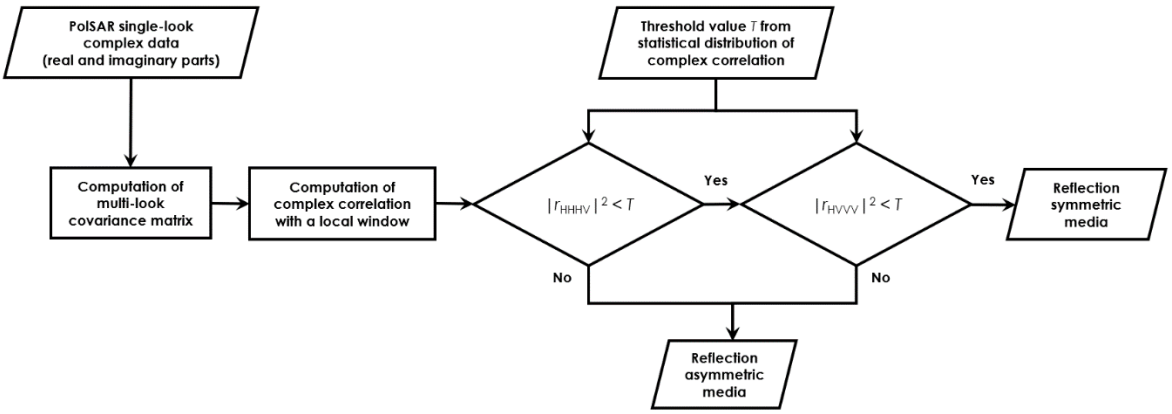

Figure 2: Reflection symmetry testing based on complex correlation coefficient, where critical value or threshold is determined from (15) with a user-specified significance level α.

a. Simulated PolSAR Data

To evaluate quantitatively the performance of multiple correlation coefficient and complex correlation coefficient for reflection symmetry testing, PolSAR simulation was carried out via Monte-Carlo procedure suggested by Lee *et al*. (1994). There were four different land cover classes in the simulation, namely, oil palm, rice paddy, rubber, and scrub-grassland. The variance-covariance statistics of the four reflection symmetric classes were extracted from the NASA/JPL AIRSAR L-band data, which were acquired over part of Kuala Muda District in Malaysia. More details about the PolSAR simulation are available in Lee (2009, Chapter 3). The number of looks under study was set to 36, 54, 72, and 90. A total of 1000 polarimetric covariance matrices were simulated for each different number of looks.

b. ALOS-2 PALSAR-2 Data

Besides simulated PolSAR data, the reflection asymmetric (or non-reflection symmetric) target detection was examined on multi-look ALOS-2 PALSAR-2 quad-polarisation data. The test data covered two separate sites in Southeast Asia: Penang and Singapore. Both the study areas were selected because of a variety of reflection symmetric and asymmetric features. Table 1 provides the details about the ALOS-2 PALSAR-2 experimental data. In this study, a 6-look (or 8-look) polarimetric covariance matrix was formed by averaging three pixels (or four pixels) in azimuth direction and two pixels in range direction.

Table 1: Specifications of ALOS-2 PALSAR-2 single-look complex data

	Penang	Singapore
Scene identifier	ALOS2096050090-160303	ALOS2452680017-221010
Acquisition date	3rd March 2016 17:30 UTC	10th October 2022 17:15 UTC
Imaging mode	Stripmap	
Orbit direction	Ascending	
Look direction	Right	
Beam number	FP6-6	FP6-4
Incidence angle at scene center	36.502°	31.083°
Radar band	L-band	
Radar frequency	1.236 GHz	
Radar wavelength	0.2424525 m	
Polarisation	Quad-polarisation (HH, HV, VH, VV)	
Line spacing	2.799 m	3.132 m
Pixel spacing	2.861 m	2.861 m
Software identifier	2.025	2.028

Results and Discussion

Table 2 lists the detection accuracy of the reflection symmetry using simulated PolSAR data based separately on multiple correlation coefficient and complex correlation coefficient. The detection accuracy is defined as a ratio of number of detected reflection symmetric covariance matrix to the total, where a unity indicates a perfect detection. Overall, the detection rates were satisfactory and confirmed the applicability of both the correlation coefficients for detecting reflection symmetry. Moreover, both showed their comparable performance under the controlled experiments, especially for the significance levels of 10^{-4} and 10^{-5}.

Figures 3 and 4 present the detection results of reflection asymmetry from multi-look ALOS-2 PALSAR-2 subscenes over Singapore and Penang, respectively. A 3×3 sliding window was used in the experiments, while the threshold was determined based on a significance level of 10^{-5}. In both the figures, the reflection asymmetric pixels detected by the multiple correlation coefficient, complex correlation coefficient, and both are separately in red, cyan, and white. Natural features, such as tree cover, grass field, and water surface, were expectably classified as reflection symmetric media. Some false detection errors appeared over the natural features when using merely either multiple correlation coefficient (i.e., red pixels) or complex correlation coefficient (i.e., cyan pixels). The combined use of both the coefficients was found to reduce significantly the undesired false alarms.

As expected, man-made objects were detected as reflection asymmetric targets, for examples, slightly oriented building, vessels, bridges, and aquaculture farms. Some buildings, vessels, and part of bridges belonging to dihedrals were categorised as reflection symmetric targets. Those buildings aligned parallel to the satellite flight direction. In agreement with Connetable *et al*. (2022), there was no

significant cross-polarised radar backscattering response from the dihedrals, resulting in no correlation between the co- and cross-polarisation channels.

Table 2: Accuracy assessment for reflection symmetry testing on simulated PolSAR data

	Oil palm		Rice paddy		Rubber		Scrub-grassland	
	MCC	CCC	MCC	CCC	MCC	CCC	MCC	CCC
36-look								
$\alpha = 10^{-3}$	0.998	0.996	0.983	0.974	0.995	0.995	1.000	0.995
$\alpha = 10^{-4}$	1.000	0.999	0.996	0.994	1.000	1.000	1.000	1.000
$\alpha = 10^{-5}$	1.000	1.000	0.999	0.998	1.000	1.000	1.000	1.000
54-look								
$\alpha = 10^{-3}$	0.996	0.995	0.973	0.961	0.993	0.992	0.997	0.996
$\alpha = 10^{-4}$	1.000	0.998	0.994	0.995	0.999	0.999	1.000	0.999
$\alpha = 10^{-5}$	1.000	1.000	1.000	1.000	1.000	1.000	1.000	1.000
72-look								
$\alpha = 10^{-3}$	0.999	0.995	0.931	0.906	0.992	0.991	0.993	0.986
$\alpha = 10^{-4}$	1.000	1.000	0.982	0.978	0.999	1.000	1.000	0.999
$\alpha = 10^{-5}$	1.000	1.000	0.995	0.997	1.000	1.000	1.000	1.000
90-look								
$\alpha = 10^{-3}$	0.991	0.988	0.902	0.887	0.982	0.985	0.992	0.985
$\alpha = 10^{-4}$	0.998	0.996	0.969	0.972	0.998	0.999	0.999	0.999
$\alpha = 10^{-5}$	1.000	1.000	0.989	0.993	1.000	1.000	1.000	1.000

Note: MCC = multiple correlation coefficient, CCC = complex correlation coefficient.

Conclusions and Recommendations

In this paper, it was shown that the recently proposed block-diagonality test statistic can be expressed in form of multiple correlation coefficient. As obtained by Connetable *et al*. (2022), the asymptotic distribution of the former under null hypothesis is a chi-squared distribution. For the latter, its square is exactly beta-distributed. Moreover, the exact distribution of the magnitude squared of complex correlation coefficient is also a beta distribution. Both the multiple correlation coefficient and complex correlation coefficient were explored for reflection asymmetric target detection from multi-look ALOS-2 PALSAR-2 L-band data. The experimental results confirmed the usefulness of reflection symmetry property of geophysical media, particularly in detecting man-made objects, such as bridges, slightly oriented buildings, vessels, aquaculture farms, *etc*. For future works, further experiments may be conducted on RADARSAT-2 C-band quad-polarisation data. In addition, statistical test for azimuth or rotation symmetry might be formulated.

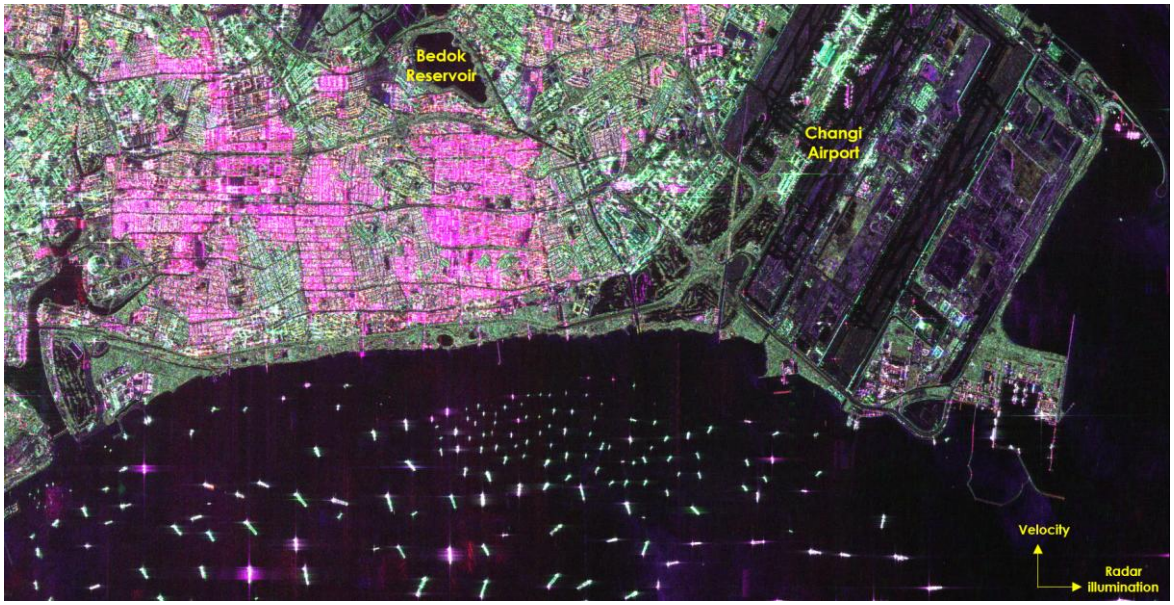

(a)

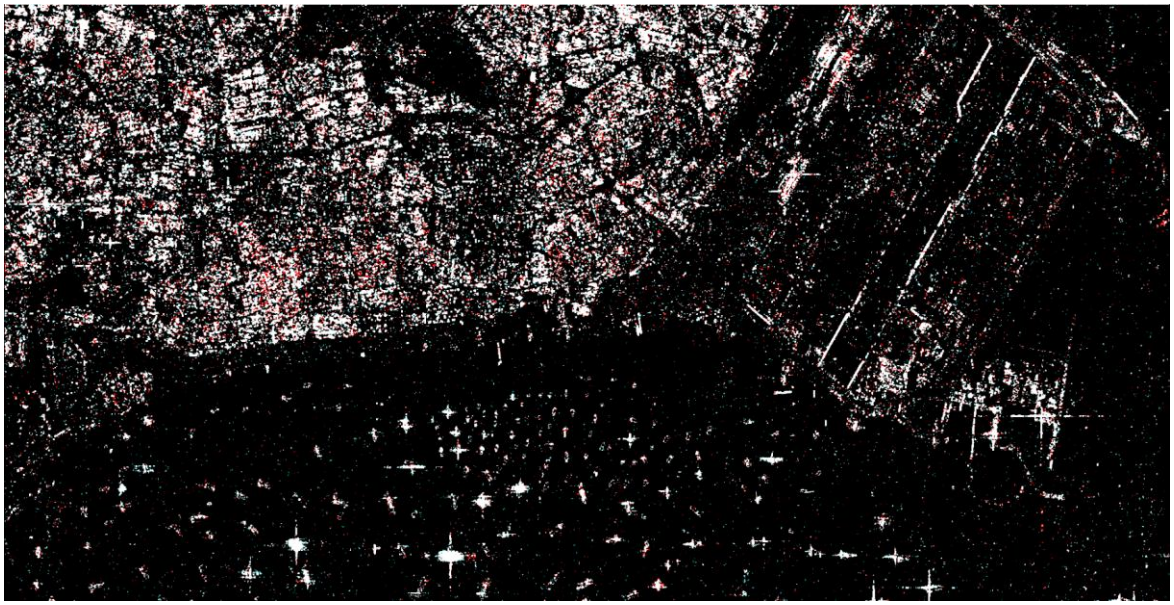

(b)

Figure 3: (a) 6-look ALOS-2 PALSAR-2 subscene over Singapore, where the HH, HV, and VV intensities are displayed in the red, green, and blue (RGB) colour space, (b) reflection asymmetry output, where the red, cyan, and white colours represent separately the reflection asymmetric pixels detected by multiple correlation coefficient, complex correlation coefficient, and both.

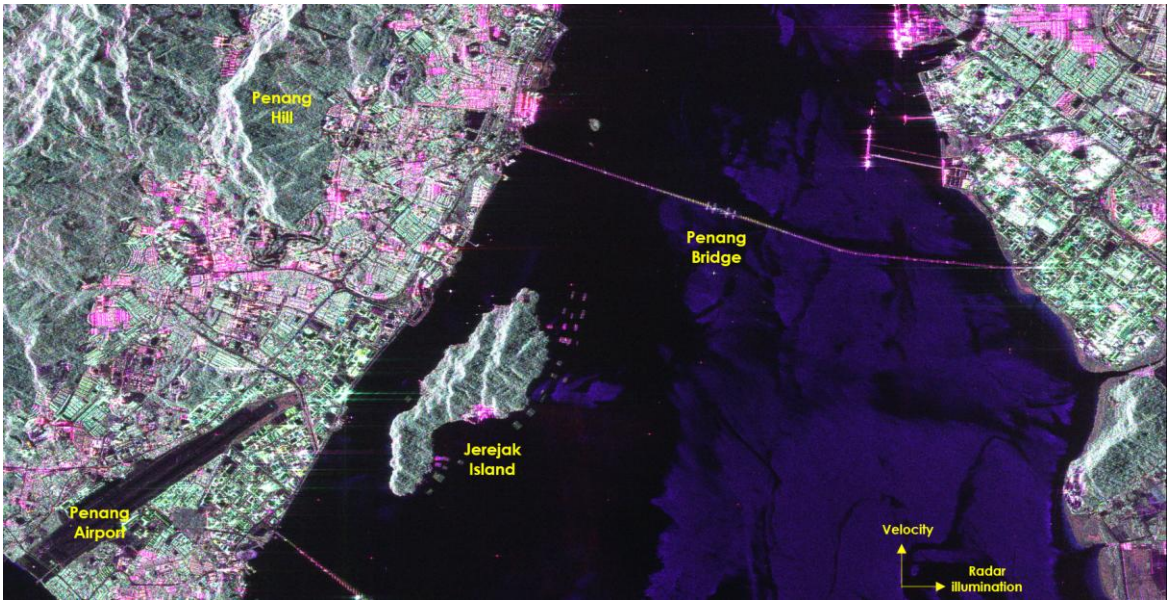

(a)

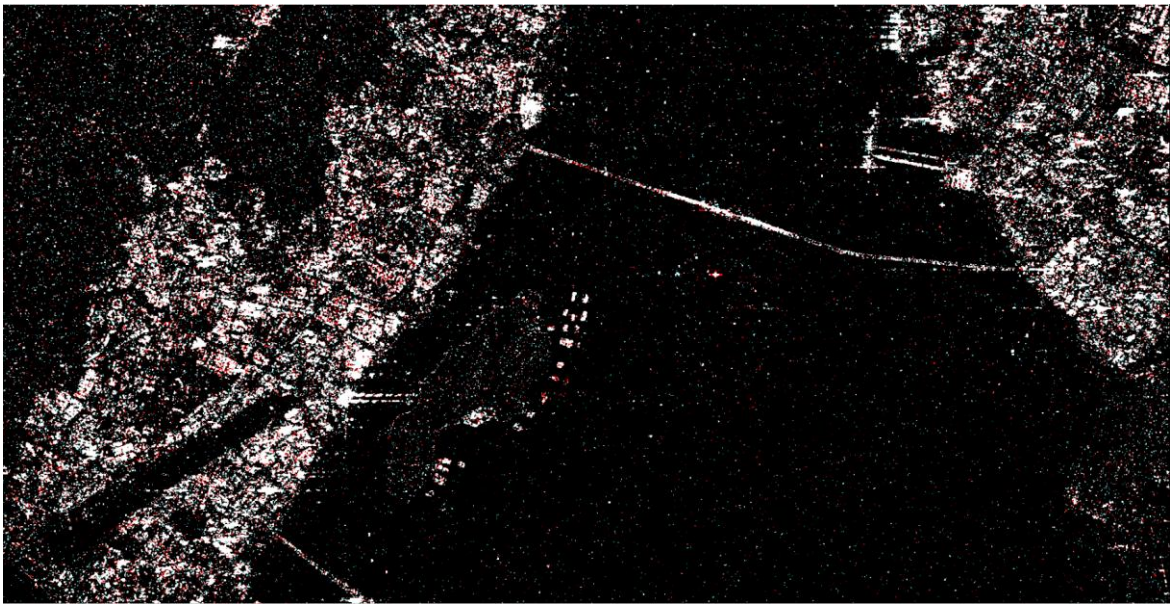

(b)

Figure 4: (a) 8-look ALOS-2 PALSAR-2 subscene over Penang, where the HH, HV, and VV intensities are displayed in the RGB colour space, (b) reflection asymmetry output, where the red, cyan, and white colours represent separately the reflection asymmetric pixels detected by multiple correlation coefficient, complex correlation coefficient, and both.

Appendices

A. Limiting Distribution of Squared Multiple Correlation

Theorem 1: Let x be beta-distributed squared multiple correlation, then $y = Lx$ follows a gamma distribution as L tends to ∞

Proof: Let $y = Lx$, then $dy = L\,dx$. Thus,

$$f(y) = \frac{\Gamma(L)}{\Gamma(L-2)L^2} y \left(1 - \frac{y}{L}\right)^{L-3}. \tag{16}$$

Given

$$\lim_{L\to\infty} \frac{\Gamma(L)}{\Gamma(L-2)L^2} = 1,$$

$$\lim_{L\to\infty} \left(1 - \frac{y}{L}\right)^{L} = \exp(-y),$$

$$\lim_{L\to\infty} \left(1 - \frac{y}{L}\right)^{-3} = 1,$$

then

$$\lim_{L\to\infty} f(y) = y\exp(-y). \tag{17}$$

It is obvious that y follows a gamma distribution with unit scale parameter and a shape parameter of 2.

B. Limiting Distribution of Complex Correlation Coefficient

Theorem 2: Let x be beta-distributed magnitude squared of complex correlation coefficient, then $y = Lx$ follows an exponential distribution as L tends to ∞

Proof: Let $y = Lx$, then $dy = L\,dx$. Thus,

$$f(y) = \frac{\Gamma(L)}{\Gamma(L-1)L} \left(1 - \frac{y}{L}\right)^{L-2}. \tag{18}$$

Given

$$\lim_{L\to\infty} \frac{\Gamma(L)}{\Gamma(L-1)L} = 1,$$

$$\lim_{L\to\infty} \left(1 - \frac{y}{L}\right)^{L} = \exp(-y),$$

$$\lim_{L\to\infty} \left(1 - \frac{y}{L}\right)^{-2} = 1,$$

then

$$\lim_{L\to\infty} f(y) = \exp(-y). \tag{19}$$

Clearly, y follows an exponential distribution with unit rate parameter.

References

H. H. Anderson, M. Højbjerre, D. Sørensen, and P. S. Eriksen (1995). *Linear and Graphical Models: For the Multivariate Complex Normal Distribution*. Springer: New York.

M. Borgeaud, R. T. Shin, and J. A. Kong (1987). Theoretical models for polarimetric radar clutter. *Journal of Electromagnetic Waves and Applications*. 1(1), pp. 73−89.

V. N. Bringi and V. Chandrasekar (2001). *Polarimetric Doppler Weather Radar*. Cambridge University Press: Cambridge.

S. R. Cloude (2010). *Polarisation: Applications in Remote Sensing*. Oxford University Press: Oxford.

P. Connetable, K. Conradsen, A. A. Nielsen, and H. Skriver (2022). Test statistics for reflection symmetry: applications to quad-polarimetric SAR data for detection of man-made structures. *IEEE Journal of Selected Topics in Applied Earth Observations and Remote Sensing*, 15, pp. 2877−2890.

A. Freeman and S. L. Durden (1998). A three-component scattering model for polarimetric SAR data. *IEEE Transactions on Geoscience and Remote Sensing*, 36(3), pp. 963–973.

Y. Fujikoshi, V. V. Ulyanov, and R. Shimizu (2010). *Multivariate Statistics: High-Dimensional and Large-Sample Approximations*. John Wiley: New Jersey.

N. R. Goodman (1963). Statistical analysis based on a certain multivariate complex Gaussian distribution (an introduction). *Annals of Mathematical Statistics*, 34(1), pp. 152–177.

N. L. Johnson, S. Kotz, and N. Balakrishnan (1994). *Continuous Univariate Distributions – Volume 2*. 2nd edition. John Wiley: New York.

J. S. Lee, M. R. Grunes, and R. Kwok (1994). Classification of multi-look polarimetric SAR imagery based on complex Wishart distribution. *International Journal of Remote Sensing*, 15(11), pp. 2299–2311.

J.-S. Lee and E. Pottier (2009). *Polarimetric Radar Imaging: From Basics to Applications*. CRC Press: Boca Raton.

K. Y. Lee (2009). *Polarimetric Synthetic Aperture Radar Image Processing for Land Cover Classification*. Singapore: Doctoral thesis, Nanyang Technological University.

G. S. Mudholkar (2006). Multiple correlation coefficient. In *Encyclopedia of Statistical Science*. 2nd edition. John Wiley: New Jersey.

S. V. Nghiem, S. H. Yueh, R. Kwok, and F. K. Li (1992). Symmetry properties in polarimetric remote sensing. *Radio Science*, 27(5), pp. 693−711.

S. V. Nghiem, S. H. Yueh., R. Kwok, and D. T. Nguyen (1993). Polarimetric remote sensing of geophysical medium structures. *Radio Science*, 28(6), pp. 1111−1130.

L. Pallotta, C. Clemente, A. De Maio, and J. J. Soraghan (2017). Detecting covariance symmetries in polarimetric SAR images. *IEEE Transactions on Geoscience and Remote Sensing*, 55(1), pp. 80−95.

S. Tahraoui, C. Clemente, L. Pallotta, J. J. Soraghan, and M. Ouarzeddine (2018). Covariance symmetries detection in PolInSAR data. *IEEE Transactions on Geoscience and Remote Sensing*, 56(12), pp. 6927−6939.

The Ohio State University Research Foundation (1952). *Effects of Type of Polarization on Echo Characteristics*. Quarterly Progress Report (No. 389-13).

J. J. van Zyl (1990). Calibration of polarimetric radar images using only image parameters and trihedral corner reflector responses. *IEEE Transactions on Geoscience and Remote Sensing*, 28(3), pp. 337−348.

S. H. Yueh, R. Kwok, and S. V. Nghiem (1994). Polarimetric scattering and emission properties of targets with reflection symmetry. *Radio Science*, 29(6), pp. 1409−1420.